Engineering Research Journal

journal homepage: https://erj.journals.ekb.eg/

Forecasting of Solar Power Generation for Experimental Dual-Axis Solar Tracker System based on ANN and FPGA Technology

Elsayed A. M. BaBars [1], Shady Y. El-Mashad [2], Saber M. Abdraboo [3], Mohamed El-sayed M. Essa [4,*]

[1] Sinai University - Faculty of Engineering- Department of Mechanical Engineering - Egypt

[2] Benha University - Faculty of Engineering at Shoubra - Department of Computer Systems Engineering - Egypt

[3] Benha University - Faculty of Engineering at Shoubra - Department of Mechanical Engineering - Egypt

[4,*] Egyptian Aviation Academy, Ministry of Civil Aviation - Institute of Aviation Engineering and Technology- Department of Electrical Power and Machines Engineering -Egypt

[*]Corresponding author E-mail: mohamed.essa@iaet.edu.eg

Abstract. This paper focuses on intelligent prediction of solar power generation from experimental solar system based on artificial neural network (ANN). The proposed hardware system is designed and implemented for dual-axis solar tracking system (DASTS). In addition, the Field Programmable Gate Arrays (FPGA) is applied to the system as the brain and core of the control system. The FPGA board is a spartan edge accelerator which equipped with the Xilinx Spartan-7 XC7S15 FPGA that gives high processing speed to enable speedy and precise alignments. The experimental hardware system is located at +31.13 ($31^{\circ}07'48''$N) and +33.8 ($33^{\circ}48'00''$ E), corresponding to the region Sinai University, Arish Campus in Arish, North Sinai, Egypt. The prediction models based ANN are compared with three types of ANNs. The ANNs algorithms are as Levenberg-Marquardt (LM), Bayesian Regularization (BR), and Scaled Conjugate Gradient (SCG). The evaluation criteria in terms of mean square error (MSE), and coefficient of determination (R^2). The data are collected from the sensors of current, voltage and solar radiation in experimental system which about 8000 samples to build the proposed forecasting model of solar power generation. These data are divided into 70% for training, 15% for validation, and 15 % for testing. The ANN forecasting models have three inputs including open circuit voltage, short circuit current, and irradiance and one output for generated power. The results indicate a high value of R^2 around 0.99 for LM, BR and SCG. However, the results show that the BR is the best ANN model with lowest MSE about 0.37 in comparing with LM and SCG with MSE about 0.4 and 2.48 respectively. Besides, the numerical and plotting results for prediction data show the superior of BR technique over other two ANN algorithm.

Keywords: Solar Power Prediction, Dual-Axis Solar Tracking, FPGA, ANN, Experimental Validation.

DOI: 10.21608/erj.2024.332639.1134

Received 31 October 2024; Received in revised form 07 December 2024; Accepted 13 December 2024

Available online 01 March 2024

1 Introduction

Indeed, the worldwide focus is shifting towards sustainable sources of energy. The technology of photovoltaic (PV) was championed as a key player in the generation of renewable energy. To elevate the productivity of PV systems, solar tracking contraptions with precise dual-axis trackers are required for solar concentrators. By dynamically regulating to the position of the sun throughout the day, DASTS can largely boost output of energy over fixed mechanisms, with research presenting potential boosts in production of 30–40%, especially in areas with high fluctuation in solar irradiance [1-3].

The effectiveness of DASTS hinges on the preciseness of the implemented algorithms of control and its capability to diminish errors of tracking. A broadly implemented methodology, Maximum Power Point Tracking (MPPT), perfects collected power of solar by recurrently aligning the orientation of PV to sustain peak output of energy under varying environmental circumstances [4-6]. Advanced techniques of adaptive control, containing ANN, fuzzy logic, and hybrid neuro-fuzzy inference systems (ANFIS), have demonstrated particular hope in improving the responsiveness of trackers of solar. Integrating ANN into systems of dual-axis has been discovered to enhance the accuracy of the response and decrease errors of tracking, resulting in a more efficient system [7-9].

The recent technological improvements, particularly in FPGA and Internet of Things (IoT) have expanded the transformation of solar tracking abilities. FPGA-based applications offer flexibility beside computational speed needed in complex algorithms of tracking. It can enhance the system accomplishment and facilitating responses in real-time to changing in solar environments [1, 10, 11]. The applying of IoT for dual axis systems has facilitated monitoring in real-time and predictive maintenance, optimizing operations and reducing downtime as shown in [12-14]. As Babars et al. in [15] presented the role of fuzzy controller in controlling DASTS based on FPGA. Besides, the integration of IoT and model predictive controllers for the DASTS are discussed in [16]. Studies contrasting conventional trackers based on sensor and trackers based on ANN accentuate the merits of advanced techniques of control. ANN regulators, as an example, provide superb preciseness in aligning with the sun, adjusting more efficiently in respect to the environmental variations than the conventional LDR-based trackers [4-5, 17]. By assimilating models of machine learning, counting both deep learning and ANN techniques, learning from environmental patterns, modern solar trackers can improve adaptive abilities and the total energy efficiency [9, 18-19].

Regardless of these ameliorations, challenges persist in developing trackers of solar energy that observe accuracy, cost and efficiency of energy. The efficient, accurate and economic of DASTS design is considered as an interesting problem of study [12-19]. As a result, our study is developed to meet these obstacles by developing an optimized DASTS that combines intelligent techniques of control with the FPGA. DASTS that are able to align PVs both horizontally and vertically are progressively identified for their capability of maximizing captured energy of solar by constantly tracking the sun's position. Past models fastened on simple designs based on sensors pointed at maximizing exposure to sunlight. Notably, Irshaidat and Soufian’s study leveraged control based on FPGA to vest both adaptability and real-time processing, thus improving response times and accuracy of tracking in trackers of dual-axis [1]. Further refinements by Hamad et al. integrated monitoring based on smart technology, which improved operational effectiveness and enabled destined diagnostics of the system [2]. Likewise, Vargas et al. designed an attainable tracker that is cost-effective in the context of education; adaptability is highlighted in technology of tracking based on two-axes for an assortment of applications [20].

Improving energy harnesses in systems of dual-axis hinges on the preciseness of algorithms of control that minimize error of tracking and sustaining optimal placement normal to the sun. MPPT has become focal to tracking of solar using preceding controllers similar to ANFIS and Type-2 fuzzy logic and to energetically counter fluctuations in irradiance of solar [8, 21]. Realizing MPPT on a much smaller scale, both Vaidianathan and Banu elucidated its effectiveness in using Arduino on systems of dual-axis, stating its feasibility for applications of cost-sensitive [6]. More ameliorated techniques of control, like control of extremum-seeking and Model Predictive Control (MPC) have also been accepted to maximize output power by regulating angles of tracking in practical [16, 19]. Creative approaches by Engin, M. and Babaei et al. in [22-23] have scouted parallel apparatuses and controllers of sliding mode enhancing the tracking systems' responsiveness under changing light circumstances. Comparative researches like those authored by Palomino-Resendiz et al. in [24], emphasized the merits of these strategies of control, which not only diminish error of tracking but also pointedly enhance efficiency of system over conventional approaches. Visions of Zhu et al. on one-axis optimized assemblies have furthered the tracking of dual-axis progression's development [25].

Techniques of artificial intelligence (AI), including ANFIS and ANN, have significantly improved systems of solar tracking by vesting adaptive practical control. ANFIS, specially, merges the strengths of fuzzy logic and neural networks, present robust executions in environments of high changeability. A survey of Guerra et al. on implementations of ANFIS in the technology of PV highlights its effectiveness to adapt to varying circumstances to sustain maximum efficient capture of solar energy [7]. Meanwhile, Jallal et al. exercised deep neural networks (DNN) to monitor trackers of dual-axis, demonstrating the potential models of data-driven to perfect the accuracy of tracking via learning continuously [18]. Hybrid AI methods, like incorporating controllers of PID and ANN have demonstrated more enhancements in tracking preciseness under varying circumstances, as showcased by Away et al. [9]. Hussieny et al. contrasted different models of AI, including GPANN, ANN, and ANFIS, discovering that hybrid models usually outperform conventional approaches in both adaptability and accuracy [17]. Research by Hadroug et al. explain how controllers of neuro-fuzzy present superb execution to systems with LDR, sustaining alignment under varying lighting circumstances [4]. Studies by Abadi et al. and Zulkornain et al. in [5,8] assure the compliance of AI-based models, with researches ensuring the effectiveness of type-2 fuzzy logic and ANFIS in controlling trackers of dual-axis solar systems.

The integration of FPGA and IoT has modified the abilities of DASTS by vesting real-time control and high-speed processing of data. The reconfigurable architecture of FPGA is especially well-appropriate for computationally intensive algorithms of tracking, as laid out by Monmasson et al., who studied its implementation in energy-based renewable [26]. Sivakumar et al. also showcased the achieved gain in efficiency of energy using FPGA-based algorithms of tracking [10]. Babars et al. furthered the development of this integration, combining FPGA with fuzzy logic control, achieving stable, accurate tracking even under varying light circumstances [15]. The technology of IoT has benefited both the maintenance of systems and destined monitoring. Ahmad and Zhang proved the potentials of IoT in making decisions based on derived data in renewable systems of energy, which improve both reliability and efficiency [27]. Sandhiya et al. developed an IoT-enabled tracker, accommodating monitoring in real-time and adaptive regulator, conditioning to conditions of weather to maximize production of energy [12]. Yusop et al. present DASTS with IoT further emphasize the technology's impact, facilitating destined diagnostics and logging of data that enhance the efficiency of the operation [13]. Babars et al. also incorporated IoT with MPC, showcasing how predictive control can perfect responses of the system to environmental variations, leading to maximum energy harnessing [16]. Al-Janab and Al-Janabi studied in [11], the implementation of IoT and FPGA in micro-grids demonstrating its effectiveness as a good solutions for renewable energy problems [11].

Studies of comparing conventional systems with sensors based on AI models for driven control to improve the behavior of DASTS are discussed in [4, 28-32].. Hadroug et al. contrasted sensors of LDR with controllers based on neuro-fuzzy concluding that the latter is superb in adaptability and accuracy to varying sunlight circumstances as shown [4]. Numerous methods of optimization, including grey control-based of sliding mode and control based fractional order (FOC), have been used to further the performance of the tracking improvements. Warrier and Shah's review of FOC in systems-based renewable cements its preciseness merits in tracking of solar [28]. In addition, Hao et al. explain optimization of solar tracking, emphasise the prominence of sophisticated control approaches in maximizing energy production [29]. Investigations by Abdelkareem and Allouhi et al. on optimizing PV and generation techniques of solar power offer necessary frameworks in the enhancement of the efficiency of the system [30- 31]. Solís-Cervantes et al. showcased the dependability of algorithms for control, which can maintain high energy production against varying sunlight circumstances [19]. Comparative studies have also valued the design of the system, as Lingala Venkateswarlu and Seshaiah's assessment of a quadrant tracker based sensor demonstrates its ability to sustain accurate energetic alignment [32]. Musa et al.'s research in time-based mechanisms of tracking emphasize the increasing trend in the direction of optimization based AI, which regularly outperforms traditional techniques [33]. Study by Taheri et al. in [34], on PV modules which is based on nanofluid utilizing tracking of dual-axis offers visions into integrating management of thermal with tracking of solar to improve efficiency of energy. In addition, a smart FPGA is suggested for grid connected direct matrix converter with integration of IoT is discussed in [35]. Finally, in this paper the introduced review envelopes the development of DASTS technology, underscoring the AI role, IoT, different algorithms of control, and FPGA in furthering system adaptability and efficiency. As a result, the main contribution of this study is to investigate an experimental hardware of dual axis solar tracker system based on FPGA. Besides, a collected data from sensors in test-rig including current, voltage and radiation are utilized to build a prediction model for solar power generation from the test-rig. The ANN is proposed to build the forecasting model, then a comparison is analyzed for three types of ANN including BR, SCG, and LM based on error metrics.

2. System Description

The practical system for the dual-axis solar tracker system was designed in one of the buildings of the Faculty of Engineering, Sinai University. The system is built on a metal structure designed to withstand solar panels and changes in wind, with various sensors such as voltage, current, and solar radiation sensors, and some cards that coordinate the transmission of signals to and from the different parts of the system, such as the Arduino Uno card and the FPGA card. Fig. 1 shows an experimental solar tracking structure designed to improve generation of energy through aligning panels of solar with the position of sun. The system includes numerous main components: (1) a panel of solar for conversion of energy, (2) a linear DC actuator for adjustment of panels, (3) an FPGA for processing signals and control actuators, (4) an Arduino Uno for acquisition of data, (5) a power supply to supply the system, and (6) sensors of LDR for detection of sunlight. These components are fixed on a robust base (7) to guarantee stability while allowing movements to be controlled. The combination of these components allows the system to dynamically regulate the panel orientation of solar for maximum generation efficiency.

The signals flow starts with the sensors of LDR, which sense the intensity of sunlight and produce analog signals (see Fig. 1). The generated signals are directed to the Arduino Uno, where they are adapted to a form of digital and transferred to the FPGA for processing. The FPGA performs as the core of control, analyzing the receiving data to decide the optimal direction for the panels of the solar. It produces signals of control, which are sent to the linear DC actuator, initiating it to regulate the position of the panels. This process permits the solar panels to always align with the trajectory of sun through the day, maximizing absorption of energy.

The functionality of system is powered through a DC power supply, guaranteeing that all elements, containing the Arduino, actuator, and FPGA, work seamlessly. This operation of closed-loop may comprise mechanisms of feedback to verify the alignment of panels and create corrections if required. By dynamically tracking the movement of the sun, the system increase the harvesting efficiency of solar energy, creating it an effective and efficient solution for applications of renewable energy.

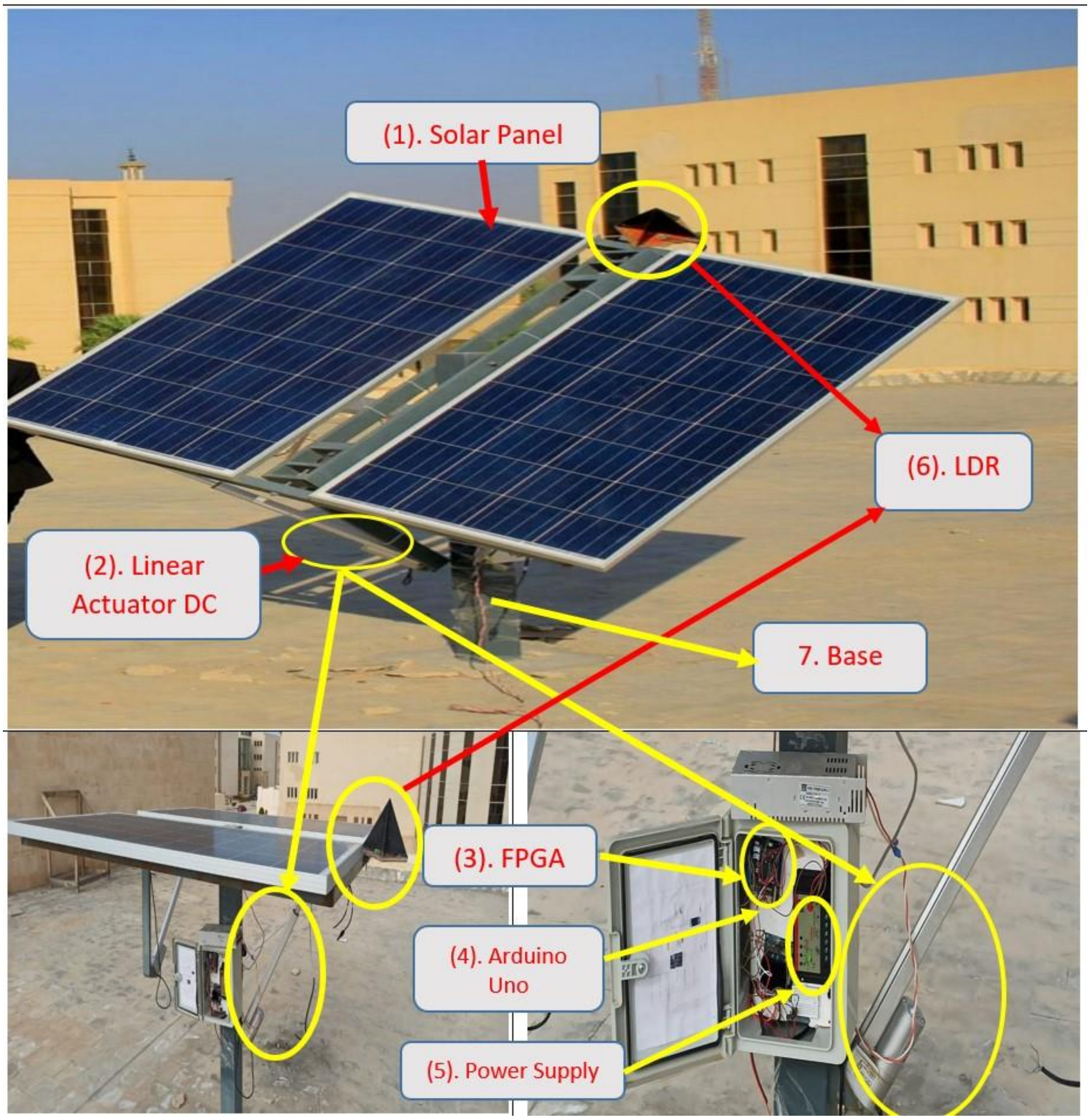

Fig. 1. Experimental Hardware test-rig for DASTS.

3. System Design

The design of the dual-axis tracking system is enhanced by different software technologies, such as analysis of loads based on ANSYS and Solidworks software packages. The calculations of the proposed system are carried out for electric linear actuators, orientation systems and tilt angles, and analysis for actuators and their selection. The calculations of stroke for choosing the linear actuator related to the axis of yaw for DC motor, which tracks the movement of the sun in east-west, were considered as will be explained later. As the tracking of yaw needs a longer stroke compared to the axis of pitch, which tracks the north-south movement of the sun, it was suggested to adopt the calculations of stroke for the yaw actuator for choosing the pitch linear actuator as well. The design is calculated as the following [36-40].

3.1 Linear Actuator Dimensions

To calculate the application of a linear actuator in a dual-axis solar tracker, we need to consider several aspects of the system, such as actuator dimensions, force, speed, and stroke. The goal is to design a mechanism that adjusts the position of the solar panel in two axes (azimuth and elevation) to track the sun efficiently. The stroke of the linear actuator determines how far it needs to extend and retract to move the solar panel through its full range of motion. We need to calculate the fully retracted and fully extended lengths based on the geometry of the system.

The lengths for accurate actuator sizing is suggested as L_1, L_2, L_3 and L_4 (see Figs. 2 and 3) based on the following specifications [36-40] as $L_1 = \frac{h}{2}$ =750 mm, $L_2 = \frac{c}{2} = 680$ mm, $L_3 = \frac{c}{20} = 68$ mm and $L_4 = \frac{h}{20} = 75$ mm. Where a, b, c, are d are width of panel, length of panel, width of frame (horizontal distance), and length of frame respectively. Moreover, h is height of pillar (vertical distance). The values of L_1, L_2, L_3 and L_4 are chosen to simplify the calculations and ensure that the actuator has enough range of motion. The design is proposed to achieve that L_1 must less than height (h) of the pillar and L_2 must less than width (c) of the frame (See Fig. 2) [36]. The 3D view of hardware regarding dimension of the system including L_1, L_2, L_3, L_4 , h and c are shown as in Fig. 2 [36]. Besides, in Fig. 3, the orientation system for minimum tilt angle and retracted is given in Fig. 3 (a), while Fig. 3 (b) show orientation system for maximum tilt angle and extended [36].

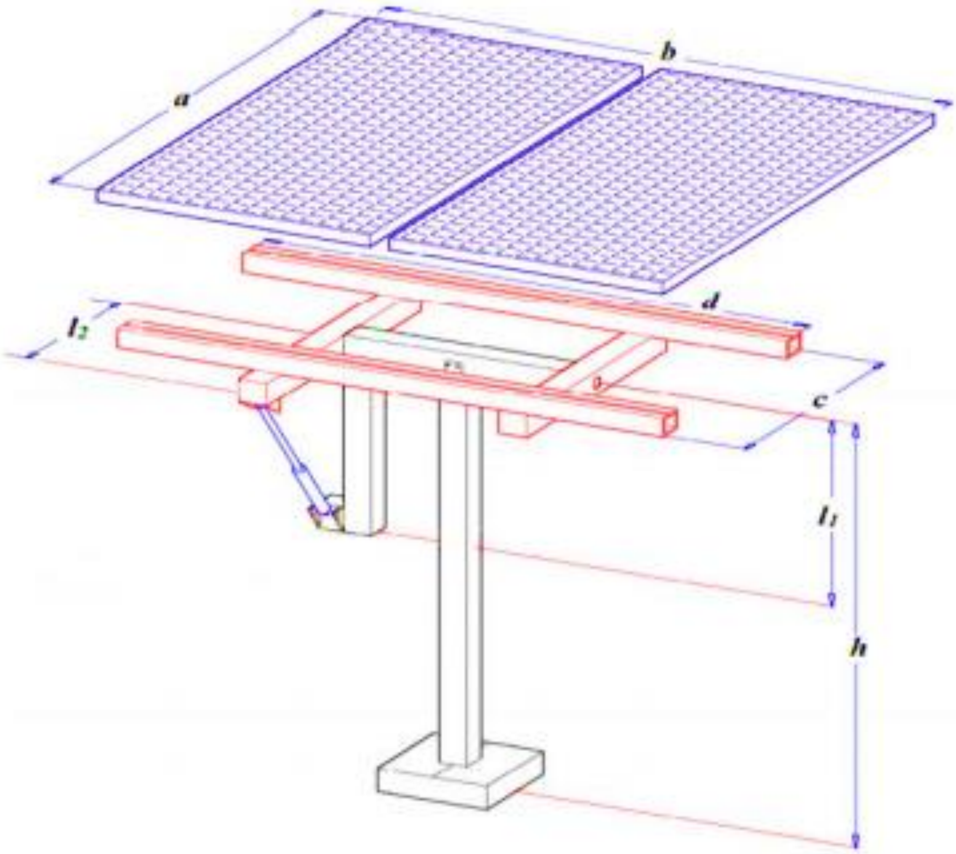

Fig. 2. 3D view of hardware system dimension.

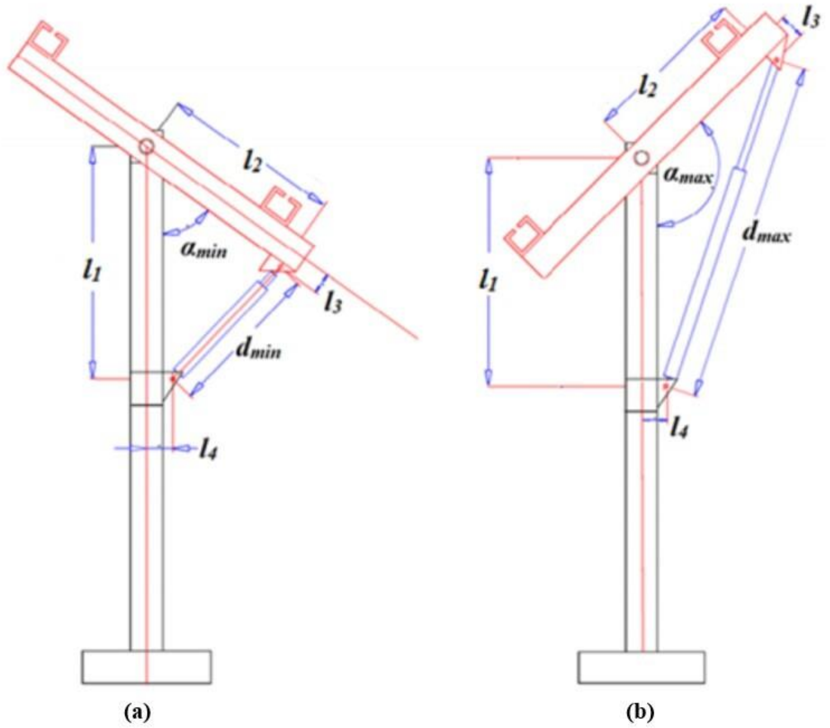

Fig. 3. (a). Orientation System for minimum tilt angle and retracted, **(b).** Orientation System for maximum tilt angle and extended.

3.2 Orientation System and Tilt Angles

The second part of the design is the orientation system for DASTS. The minimum tilt angle of the solar panel (α_{min}) is defined as the initial angle between the support frame and vertical axis. In the design for symmetry, the maximum tilt angle, $\alpha_{max} = \pi - \alpha_{min}$ (determined by symmetry), with angle α_{min} ranging from 0 to $\frac{\pi}{2}$. The calculation of minimum tilt angle is depicted in Fig. 4. (a), while the calculation of maximum tilt angle is given in Fig. 4 (b) [36].

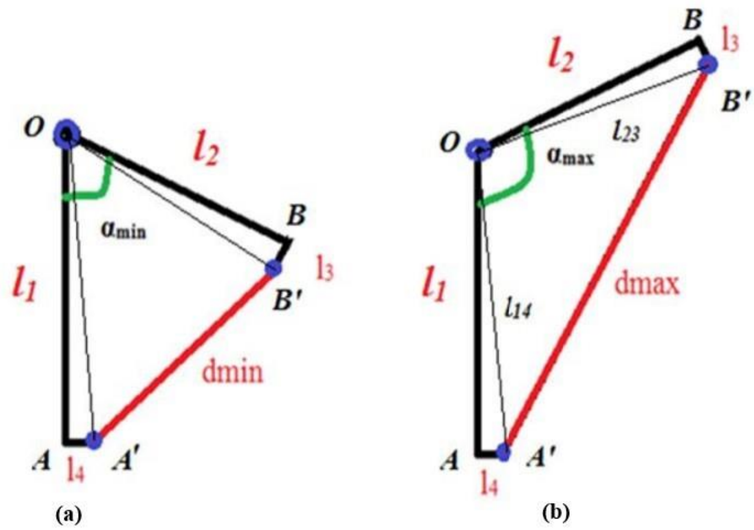

Fig. 4. (a). Calculation of minimum tilt angles, **(b).** Calculation of maximum tilt angles.

3.3 Dimension Calculations for Linear Actuator

The third part of the design is used to optimal calculations for linear actuators length that suitable for the DASTS movement (See Figs. 3 and 4). The actuator lengths is chosen as fully retracted length is d_{min} and fully extended length is d_{max} . The lengths are calculated based on initial angle α_{min} and using the following formula as in Equations (1) and (2). In fact, d_{min} represents the shortest distance when the actuator is fully retracted, corresponding to the smallest tilting angle α_{min}. While d_{max} represents the longest distance when the actuator is fully extended, corresponding to the largest tilting angle α_{max}.

$$d_{min}^2 = OA'^2 + OB'^2 - 2 \cdot OA' \cdot OB' \cdot \cos(\alpha_{min} - A\hat{O}A' - B\hat{O}B') \quad (1)$$

$$d_{max}^2 = OA'^2 + OB'^2 - 2 \cdot OA' \cdot OB' \cdot \cos(\pi - \alpha_{min} - A\hat{O}A' - B\hat{O}B') \quad (2)$$

The values of lengths are selected in this paper as d_{min} = 895 mm (fully retracted length), d_{max} = 1788 mm (fully extended length). These values are derived based on the geometry of the solar tracking system, which includes the lengths L_1, L_2, L_3 and L_4 and the angles α_{min} and α_{max} . The selection of actuators is applied based on calculations, with the following parameters as stroke is 24 inches, input voltage is 12 VDC, speed is 0.3 inch/s, maximum force is 400 lb, retracted Length is 24 inches and extended length is 48 inches.

3.4 Design Analysis

The linear actuator needs to provide enough force to move the solar panel through its range of motion. The actuator force is calculated based on the torque required to rotate the solar panel about its axis of rotation, taking into account external forces such as the weight of the panel, wind, and inertia. The analysis for the suggested design is performed for force and torque on the tracking system (See Fig. 5). The details of the analysis is described based on actuator torque (M_{act}) (See Equation 3) at the center of rotation, eccentric moment (M_e) (See Equation 4), wind moment (M_{wind}) (See Equation 5), as depicted in Equations (3), (4) and (5). Fig. 6 demonstrates the optimal calculation of maximum and minimum tilt angles and retracted and extended length of linear actuator [36]. The torque provided by the actuator is the sum of the following moments:

$$M_{act} = F_1 \cdot L_3 + F_2 \cdot L_2 = F \cdot (\cos(\theta) \cdot L_3 + \sin(\theta) \cdot L_2) \quad (3)$$

$$M_e = m \cdot g \cdot \cos(\alpha) \cdot e \quad (4)$$

Where: F_1 and F_2 are forces applied by the actuators while L_3 and L_2 are the lengths of the actuator arms. In addition, m stands for weight of solar panels, e is eccentricity, the distance between center of panel and rotation axis, perpendicular to the panel and α is defined as angle between panel and vertical axis. θ represents the angle between the linear actuator's direction and the horizontal plane or a reference line, while, M_e is an eccentric moment.

$$M_{wind} = C_m \cdot 0.613 \cdot v_{wind}^2 \cdot A \cdot b1 \quad (5)$$

Where, C_m is the wind momentum coefficient, , v_{wind} stands for wind speed in m/s, A is the panel surface area, and b1 is the width of the solar panel perpendicular to the axis.

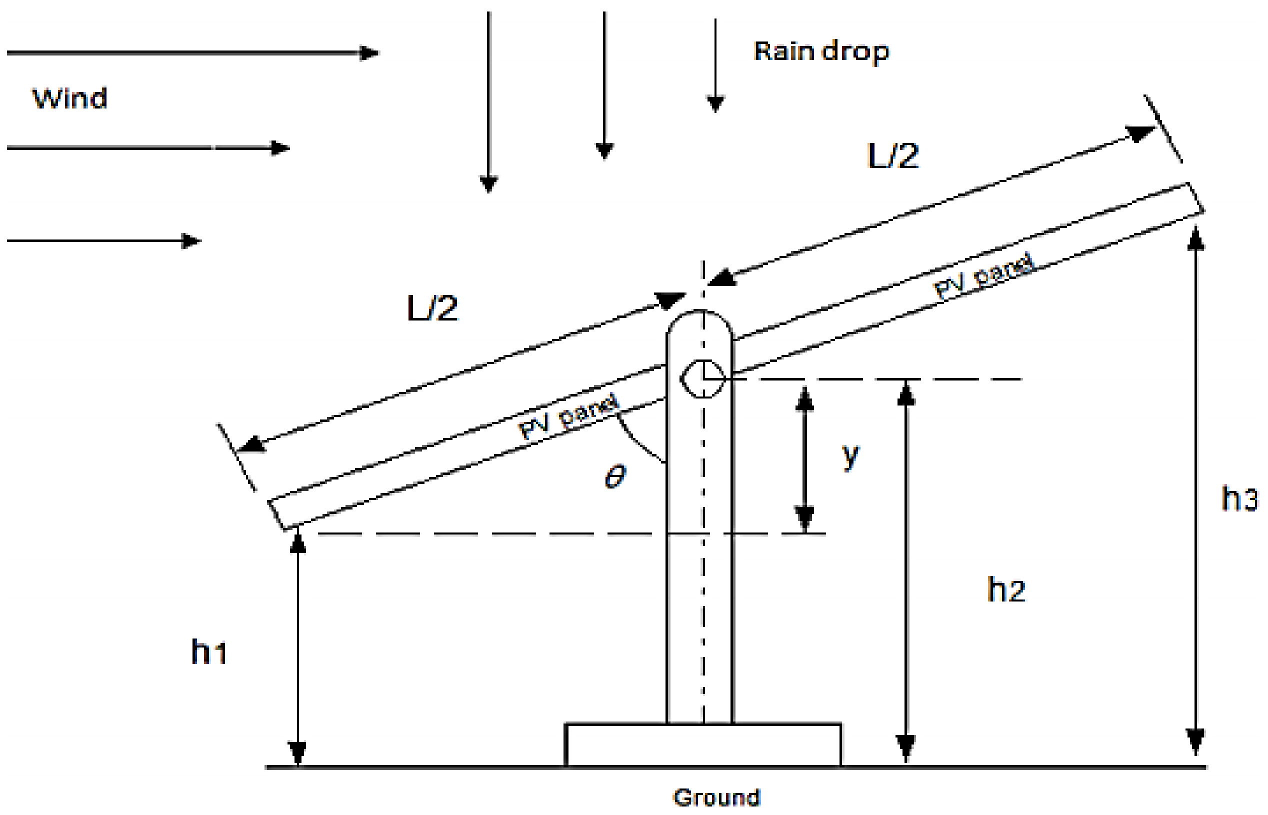

Fig. 5. Front view of hardware system dimension.

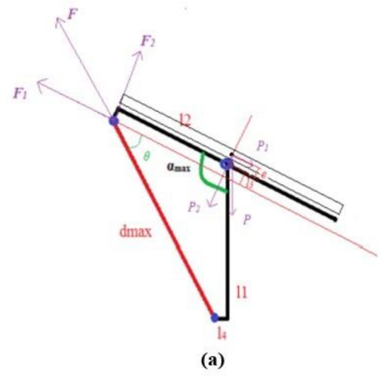

Fig. 6. (a). Optimal Calculations for maximum tilt angles and extended for Linear Actuators Length, **(b).** Optimal Calculations for minimum tilt angles and retracted for Linear Actuators Length.

3.5 Dynamic Behavior

For a more detailed analysis, the moment of inertia of the solar panel and the actuator system is taken into consideration, and calculate the angular acceleration using the Equation 6. The friction and inertia for the system is studied based on neglecting the friction torque at roller bearings (points $\mathrm{O}, \mathrm{A}'$and B') (See Figs. 4 and 6).

$$\mathrm{M_{qt}} = \mathrm{J} \cdot \mathrm{e_{MAX}} \tag{6}$$

Where $\mathrm{e_{MAX}}$ is defined as maximum angular acceleration, and J is the moment of inertia. Finally in the analysis, the torque balance equations is calculated based on total torque ($\mathrm{M_{qt}}$) for system balance as presented in Equation (7).

$$\mathrm{M_{qt}} = \mathrm{M_{act}} - \mathrm{M_e} - \mathrm{M_{wind}} \tag{7}$$

This analysis ensures the actuator chosen meets the requirements for tilt angle, force, and rotational stability under external conditions like wind. This structured approach can guide actuator selection and mechanical design optimization for dual-axis solar trackers. The rendered 3D assembly for the mechanical frame is given in Fig. 7.

Fig. 7. Rendered 3D Assembly of the Mechanical Frame.

4. Artificial Neural Network (ANN)

ANNs are considered as computational representations envisioned by the structure of neural for the brain of humans, involving connected nodes, also called neurons, structured in layers. Via a process of training, ANNs learn to identify patterns and produce predictions, regulating their weights and numerical biases founded on data of input to enhance accuracy. This flexibility makes the models of ANNs perfect for users that demand complex making of decision, responses in real-time and adaptive control tasks that are interesting for conventional programming due to the variable and nature non-linear of real-world data. In vigorous environments such as tracking of the sun, where conditions vary and fluctuate repeatedly, ANNs are especially beneficial due to their capability for learning based on continual and self-optimization [7, 18]. The using of ANN and FPGA in a DASTS is considered the main core of this study for prediction process of generated power. This improves the ability of the system to react accurately to environmental variations, presenting merits over conventional systems of control. The suggested structure of the ANN model is given in Fig. 8. The performance metrics for the ANN models are depicts in Equations 8 and 9 [41].

The evaluation of the suggested prediction ANN structure is tested using the two metrics: mean square error (MSE), and coefficient of determination (R^2) (see Equations 8 and 9). These criteria is used to test the performance of ANNs. As well, the value of R^2 =1, shows an excellent fit and R^2 near 1 refer to a good fit. Consequently, it is very clear that the values of R^2 is proportional to the fitting quality.

$$MSE = \sqrt{\frac{1}{n}\sum_{i=1}^{n}(P_{ANN} - P_{actual})^2} \quad (8)$$

$$R^2 = 1 - \frac{\sum_{i=1}^{n}(P_{ANN} - P_{actual})^2}{\sum_{i=1}^{n}(P_{ANN} - P_{ANN-mean})^2} \quad (9)$$

Where, n is the number of samples, P_{ANN} is forecasting power-based ANN, P_{actual} represents actual collected power, and $P_{ANN-mean}$ is mean of predicting power-based ANN.

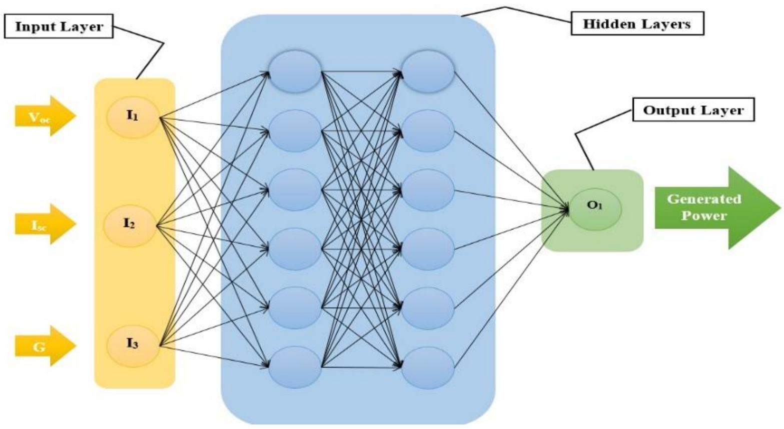

Fig. 8. Proposed Structure of ANN model.

5. Results and Discussion

The dataset of 8000 samples is collected from current, voltage, and solar radiation sensors in the experimental DASTS test-rig. Besides, the data are collected for different days to cover most of cases for variations in the environment. The results in this paper used the concept of analyzing the performance of the study through different visualizations such as comparison charts, plots, and numerical tables, which can give valuable insights. In general, the plots of regression is used to demonstrate how well the forecasted outputs match the measured values, while histograms of error will highpoint the distribution of forecasting errors through the dataset, facilitating to recognize of any biases or patterns in the performance of the obtained model. The evaluation based comparison will offer a clearer image of the accuracy of the obtained model and areas for additional improvement.

In this paper, the ANN is used to build a prediction model for the generated power from experimental DASTS based on three measured inputs, including open circuit voltage, short circuit current, and irradiance. As mentioned, the ANN have three inputs and one output for generated power. The collected dataset is divided into three parts, like 70%, 15% and 15%, for training, validation, and testing, respectively. This mean that the used samples for training is about 5600 sample, 1200 samples for validation and 1200 for testing. Besides, 90 samples are used to evaluate the ANN models in prediction phase. The ANN models are built based on three algorithms such as LM, BR, and SCG. The proposed models is built based on 50 hidden layer (see Fig. 9). Tables 1 and 2 show the evaluation performance for the proposed models of ANN in different criteria. Besides, Fig. 10 demonstrates an evaluation performance in chart shape. In addition, Fig. 11 demonstrates regression in training of ANN based on BR as in Fig. 11 (a), regression in testing of ANN based on BR as shown in Fig. 11 (b), and regression of all output for ANN based on BR as presented in Fig. 11 (c). The training performance for the BR is depicted in Fig. 12. Moreover, Fig. 13 presents MSE with epoch relation for training as in Fig. 13 (a), MSE with epoch relation for testing, and the MSE with epoch relation for validation as in Fig. 13 (c). The error histogram is given in Fig. 14. Besides, the training state for BR algorithm is shown in Fig. 15. Finally, the regression for predicted solar power based on the BR algorithm is presented in Fig. 16 and Fig. 17 shows the error histogram for predicting solar power generation.

The results show that both the LM and BR algorithms executed well in the prediction of generated power of the solar system, with high correlation of determination (R^2) and low Mean Squared Errors (MSE) across phases of prediction, training, testing, and validation (see Figs. 11-15). However, BR marginally outperformed LM in terms of accuracy of forecasting power, giving the lowest forecasting MSE of 0.37 and preserving high consistency through all phases (see Tables 1 and 2). In contrast, the SCG technique had a higher MSE, signifying it may be less appropriate for accurate power prediction from DASTS. Therefore, BR is recommended as the best method for the power prediction from the solar system due to its superior forecasting stability and accuracy across data of testing, validation, and testing (see Figs. 16 and 17).

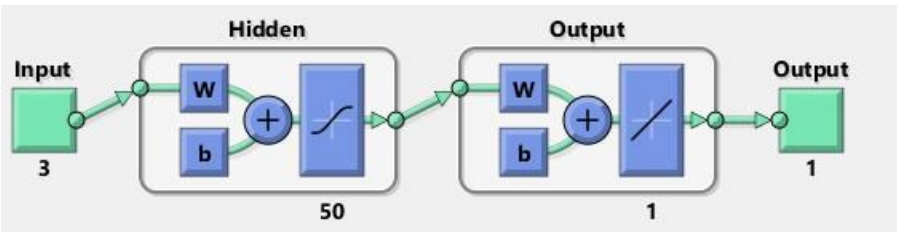

Fig. 9. Matlab Structure of ANN with tuned parameters.

Table 1. Evaluation Performance of ANN Models

Methods	Training of ANN Model		Validation of ANN Model		Testing of ANN Model		Prediction of ANN Model	
	R^2	MSE	R^2	MSE	R^2	MSE	R^2	MSE
LM	0.998	2.23	0.998	2.25	0.998	2.23	0.999	0.4
BR	0.998	2.28	1	1	0.998	2.13	0.999	0.37
SCG	0.997	3.37	0.997	3.32	0.997	3.57	0.998	2.48

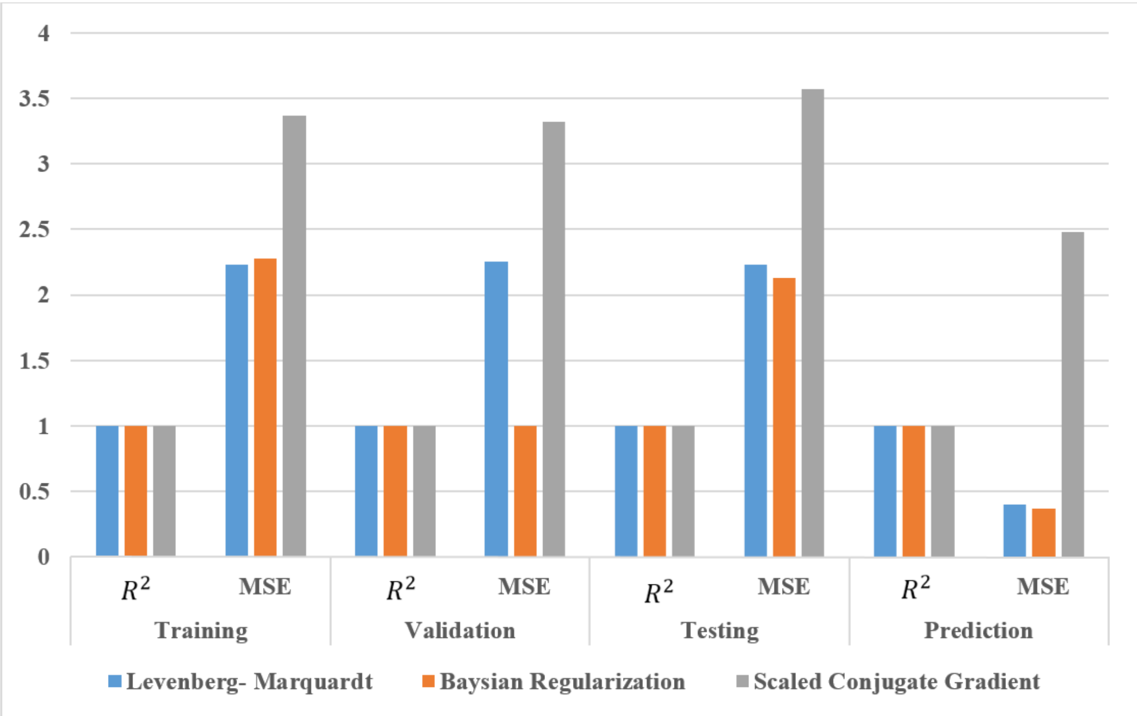

Fig. 10. Comparison chart of various ANN Model.

Table 2. Comparison of ANN Models.

Methods	Epoch	Time	Performance	Gradient	MU	Validation Check
LM	73	0.04	2.23	0.426	0.001	6
BR	748	0.55	2.29	0.0045	5×10^{10}	---
SCG	164	0.03	3.37	7.21	---	6

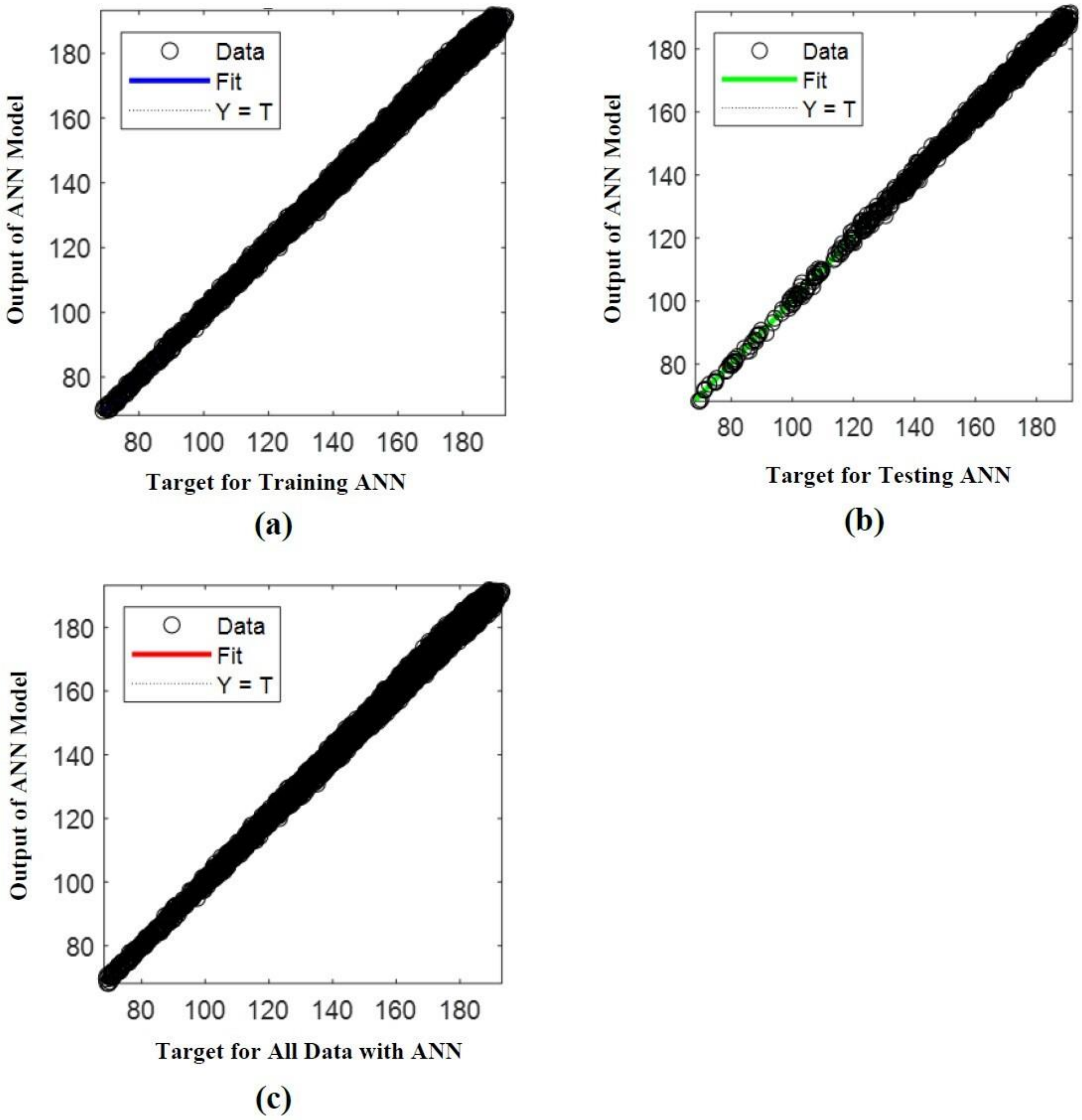

Fig. 11. (a). Correlation for training of ANN based on BR **(b).** Correlation for testing of ANN based on BR **(c).** Correlation of all output for ANN based on BR.

Fig. 12. Best Training Performance for Baysian Regulation Algorithm.

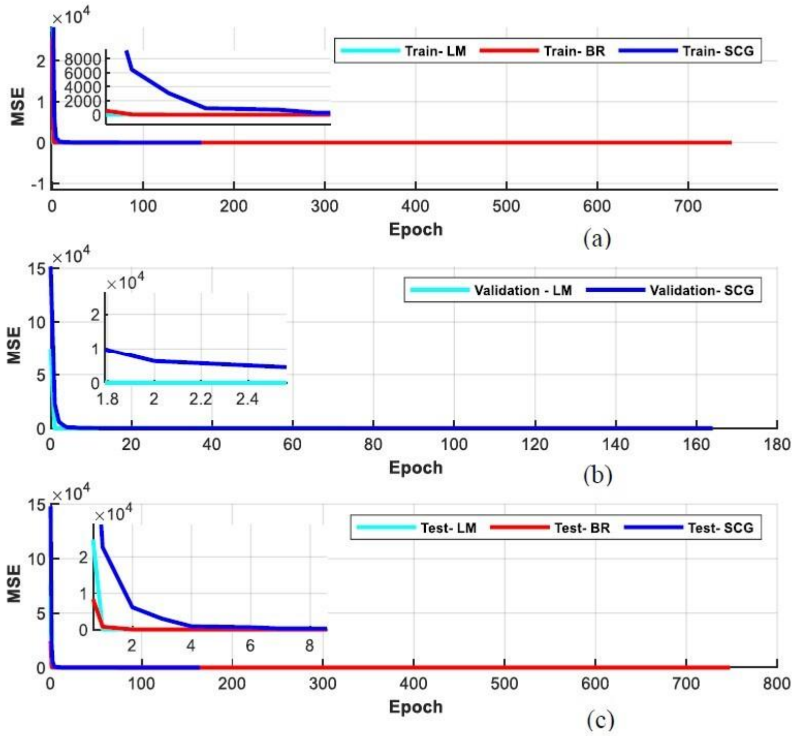

Fig. 13. (a). MSE with Epoch relation for Training, **(b).** MSE with Epoch relation for Testing, **(c).** MSE with Epoch relation for Validation.

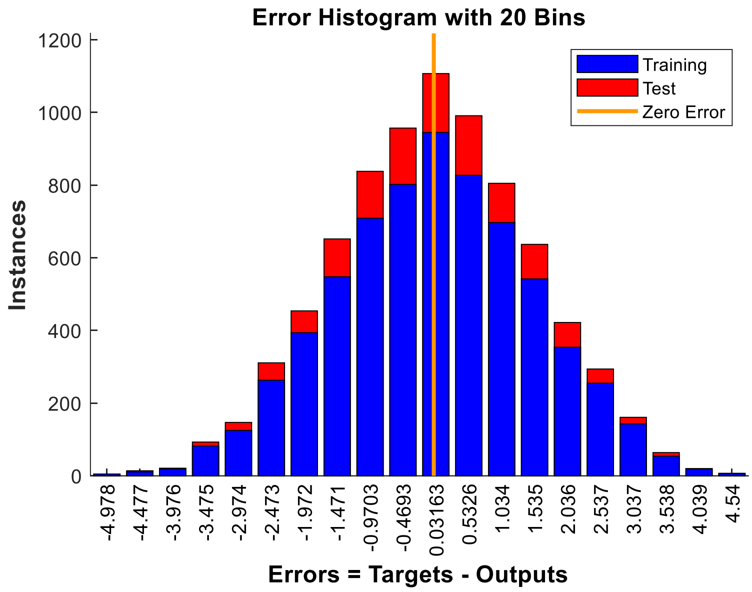

Fig. 14. Error Histogram for BR Algorithm.

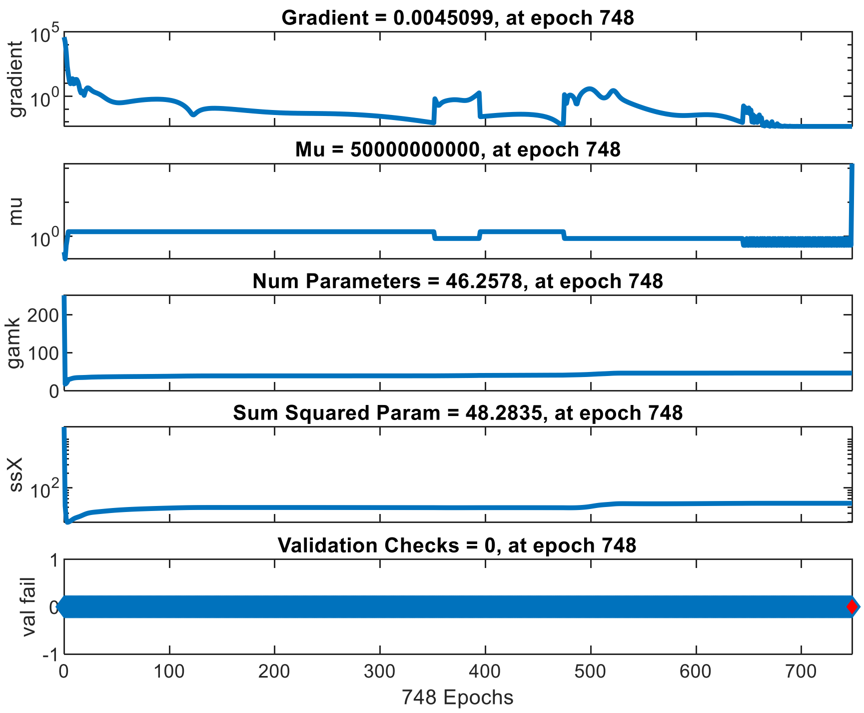

Fig. 15. Training State for BR Algorithm.

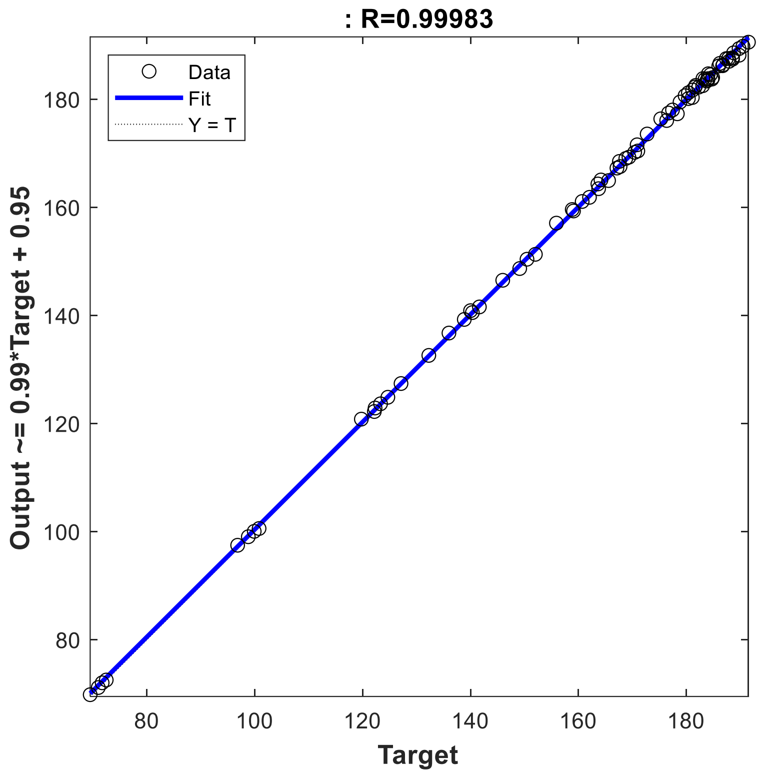

Fig. 16. Regression of Predicted Power based on BR Algorithm.

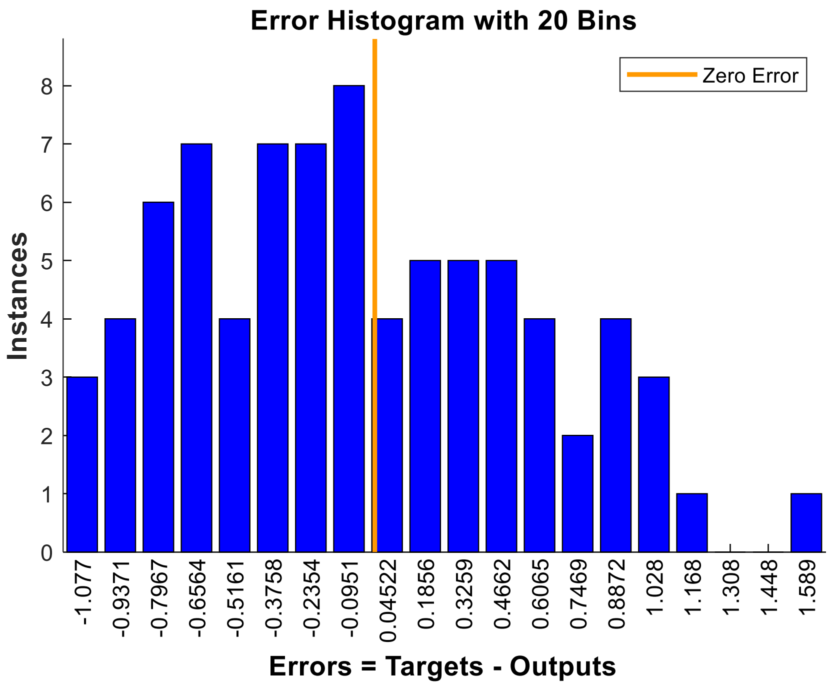

Fig. 17. Error Histogram of Predicted Power based on BR Algorithm.

Conclusion

The design and analysis of the DASTS system are discussed in this paper in detail. The FPGA card is used in the test-rig as the brain of the system, which receives signals from sensors then processing data to give the suitable decision for the actuators. In this paper, three ANN models are built based on LM, SCG, and BR algorithms. The dataset of data is collected from the experimental hardware of the solar system based on managing the data using FPGA board. The three algorithm are compared based on different performance tests such as MSE and R. BR marginally outperformed LM in terms of accuracy of forecasting power, giving the lowest forecasting MSE of 0.37 and preserving high consistency through all stages. Therefore, BR is recommended as the best algorithm for the power prediction from DASTS due to its superior forecasting stability and accuracy across different data stages. The key points of the paper could summarized as follows:

- Implementing an experimental hardware for DASTS system based on FPGA.
- Successfully collected data from current, voltage, and radiation sensors creating an acceptable dataset for building the model.
- Investigated and optimized ANN algorithm, attaining high accuracy in prediction of solar power generation.
- The BR model effectively predict the generated power based on the performance tests.

Acknowledgement

The authors would like to extend their sincere thanks and appreciation to the Academy of Scientific Research and Technology (ASRT), Cairo, Egypt, for their assistance, advice, and provision of the components required to complete this research.

List of Nomenclature

Symbol	Definition
A	Surface area of the solar panel.
a	Width of panel
b	Length of panel
b1	Width of the solar panel relative to the rotation axis.
c	Width of the frame (horizontal distance).
C_m	Coefficient of wind moment (typically 0.6 for maximum resistance).
d	Length of frame
$\mathrm{d}_{\mathrm{min}}$	Fully retracted length of the linear actuator.
$\mathrm{d}_{\mathrm{max}}$	Fully extended length of the linear actuator
e	Eccentricity (distance from the center of the panel to the center of rotation).
F	Force provided by the actuator
h	Height of the pillar (vertical distance).
J	Moment of inertia of the rotating parts.
$\mathrm{L}_1, \mathrm{L}_2, \mathrm{L}_3, \mathrm{L}_4$	Actuator lengths
M_{act}	Actuator torque
M_e	Eccentric moment due to the weight of the solar panel.
M_{wind}	Wind moment acting on the solar panel.
n	Number of samples

P_{ANN}	Forecasting power-based ANN
P_{actual}	Actual collected power
$P_{ANN-mean}$	Mean of predicting power-based ANN.
R^2	Coefficient of determination
V_{wind}	Wind speed

List of Greek Symbols	
Symbol	**Definition**
θ	The angle between the linear actuator's direction and the horizontal plane or a reference line.
α	Tilt angle of the solar panel relative to the vertical axis
α_{min}	Minimum tilt angle of the solar panel.
α_{max}	Maximum tilt angle of the solar panel

List of Acronyms

Acronym	**Full Form**
ANN	Artificial Neural Network
ANFIS	Adaptive Neuro-Fuzzy Inference System
BR	Bayesian Regularization
CPV	Concentrated Photovoltaic
DASTS	Dual-Axis Solar Tracking System
DNN	Deep Neural Network
FPGA	Field Programmable Gate Array
FOC	Fractional Order Control
GRNN	General Regression Neural Network
GPANN	Generalized Polynomial Artificial Neural Network
IoT	Internet of Things
LM	Levenberg-Marquardt
LDR	Light Dependent Resistor
MPPT	Maximum Power Point Tracking
MSE	Mean Square Error
PID	Proportional-Integral-Derivative
PV	Photovoltaic
SCG	Scaled Conjugate Gradient

References

1. Irshaidat, M., Soufian, M.: A FPGA Implementation of a Dual-Axis Solar Tracking System," in: 12th International Conference on Developments in eSystems Engineering (DeSE), pp. 970-974. Kazan, Russia (2019).

2. Hamad, B., Ibraheem, M., Abdullah, A.: Design and Practical Implementation of Dual-Axis Solar Tracking System with Smart Monitoring System. Przeglad Elektrotechniczny 96(10), 99–110(2020).

3. Mamajonov, X., Madaminov, M.: Advancements in solar technology: dual axis solar tracking systems. TADQIQOTLAR. *UZ* 32 (1), 32–38 (2024).

4. Hadroug, N., Iratni, A., Hafaifa, A. Boudjemline, O., Alshammari, H. Jerbi, I., Colak, Chen, X.: Energy efficiency improvement in photovoltaic installation using a twin-axis solar tracking mechanism with LDR sensors compared with neuro-fuzzy adaptive inference structure. Journal of Electrical Engineering & Technology 18(4), 2943-2967 (2023).

5. Zulkornain, M., Noor, S., Rahman, H., Musa, S.: The Analysis of Dual Axis Solar Tracking System Controllers Based on Adaptive Neural Fuzzy Inference System (ANFIS). Journal of Mechanical Engineering 20(2), 99–110 (2023).

6. Banu, M., Vaidianathan, B.: Maximum Power Point Tracking Dual Axis Solar Panel Using Arduino. in: UNO, vol. 99, pp. 1–13. (2024).

7. Guerra, M., de Araújo, F., de Carvalho Neto, J., Vieira, R.: Survey on adaptive neural fuzzy inference system (ANFIS) architecture applied to photovoltaic systems. Energy Systems 15(2), 505–541 (2024).

8. Abadi, I., Uyuniyah, Q., Fitriyanah, N., Jani, Y., Abdullah, K.: Performance study of maximum power point tracking (MPPT) based on type-2 fuzzy logic controller on active dual axis solar tracker. in: E3S Web of Conferences, vol. 190, pp. 00016. (2020).

9. Away, Y., Novandri, A., Raziah, I., Melinda, M.: A New Technique for Improving the Precision of Dual-Axis Tetrahedron-Based Sensor With Switching Between PID and ANN. IEEE Access 11, 89138–89151 (2023).

10. Sivakumar, V., Vimal, S., Vadivel, M., Baskar, V.: FPGA based efficiency improvement of renewable integrated power system using advance power tracking algorithm. in: AIP Conference Proceedings, vol. 2519 (1). (2022).

11. Al-Janab, I., Al-Janabi, S.: Smart micro-grid model to generate renewable energy based on embedded intelligent and FPGA. in: Recent Advances in Material, Manufacturing, and Machine Learning, CRC Press, pp. 278–293. (2023).

12. Sandhiya, B., Raja, S., Raja, R., Ethiraj, M., Rasool, M.: Internet of Things based dual axis solar tracking system. in: AIP Conference Proceedings, vol. 2802(1). (2024).

13. Yusop, A., Shabri, M., Sulaiman, N., Khamil, K., Mohammed, R., Sultan J.: Development and evaluation of dual axis solar tracking system with IoT data monitoring. Przegląd Elektrotechniczny 99 (1) 28–32, (2023).

14. Motlagh, N., Mohammadrezaei, M., Hunt, J., Zakeri, B.: Internet of Things (IoT) and the energy sector. Energies 13(2) 4–9, (2020).

15. Babars S., El-Mashaad, S., Abdraboo, S., Essa, M.: Modeling and Control of an Experimental Fuzzy Logic Controlled Dual Axis Solar Tracking System based on Field Programmable Gate Array. Int. J. Appl. Energy Syst. 6(2) 53–64, (2024).

16. Babars S., El-Mashaad, S., Abdraboo, S., Essa, M.: Design of Model Predictive Control and IoT for Experimental Dual Axis Solar Tracker System based on FPGA. Int. J. Appl. Energy Syst. 6(2) 53–64, (2024).

17. Hussieny, O., El-Beltagy, M., El-Tantawy, S.: Forecasting of renewable energy using ANN, GPANN and ANFIS (A comparative study and performance analysis). in: 2nd Novel Intelligent and Leading Emerging Sciences Conference (NILES), 2020, pp. 54–59. (2020)

18. Jallal, M., Chabaa, S., Zeroual, A.: A novel deep neural network based on randomly occurring distributed delayed PSO algorithm for monitoring the energy produced by four dual-axis solar trackers. Renewable Energy 149, 1182–1196, (2020).

19. Solís-Cervantes, C., Palomino-Resendiz, S., Flores-Hernández, D., Peñaloza-López, M., Montelongo-Vazquez, M.: “Design and Implementation of Extremum-Seeking Control Based on MPPT for Dual-Axis Solar Tracker,” Mathematics 12(12) 1–9, (2024).

20. Vargas, A., Francisco, G., Montezuma, M., Sampaio, P., Acho, L.: Low-cost dual-axis solar tracker with photovoltaic energy processing for education,″ Sustainable Energy Technologies and Assessments 53, 102–142, (2022).

21. Imron, C., Abadi, I., Akbar, I., Maknunah, J., Nor, A., Uyun, A.: Performance Comparison of the Single Axis and Two-Axis Solar System using Adaptive Neuro-Fuzzy Inference System Controls. in: E3S Web of Conferences, vol. 190, p. 00005, EDP Sciences, (2020).

22. Engin, M.: Controller Design for Parallel Mechanism Solar Tracker. Machines 11(3) 3–72, (2023).

23. Babaei, S., Yahyazadeh, M., Marj, H.: Novel MPPT for Linear-Rotational Sun-Tracking System Using Fractional Fuzzy Grey-Based Sliding Mode Control. Iran. J. Sci. Technol. Trans. Electr. Eng. 44(4) 1379–1401, (2020).

24. Palomino-Resendiz, S., Cadix-Martín, V., Al-Hadithi, B., Flores-Hernández, D.: Comparative analysis of control strategies for the reduction of tracking error in CPV systems. in: AIP Conference Proceedings, vol. 2841(1), (2023).

25. Zhu, Y., Liu, J., Yang, X.: Design and performance analysis of a solar tracking system with a novel single-axis tracking structure to maximize energy collection. Applied Energy 264 114–647, (2020).

26. Monmasson, E., Hilairet, M., Spagnuolo, G., Cirstea, M.: System-on-chip FPGA devices for complex electrical energy systems control. IEEE Industrial Electronics Magazine 16(2) 53–64, (2021).

27. Ahmad, T., Zhang, D.: Using the internet of things in smart energy systems and networks," Sustainable Cities and Society 68 102–783, (2021).

28. Warrier, P., Shah, P.: Fractional Order Control of Power Electronic Converters in Industrial Drives and Renewable Energy Systems: A Review. IEEE Access 9 58982–59009, (2021).

29. Hao, D., Qi, L., Tairab, A., Ahmed, A., Azam, A., Luo, D., Pan, Y., Zhang, Z., Yan, J.: Solar energy harvesting technologies for PV self-powered applications: A comprehensive review. Renewable Energy 188 678–697, (2022).

30. Allouhi, A., Rehman, S., Buker, M., Said, Z.: Up-to-date literature review on Solar PV systems: Technology progress, market status and R&D, Journal of Cleaner Production 362 13–33, (2022).

31. Abdelkareem, M.: A Survey Paper: Electrical and Orientation Techniques for Generating PV Solar Power. Journal of Cleaner Production 365 13–23, (2020).

32. Lingala, C., Seshaiah, T.: Dual sun tracking system by using four quadrant sensor. Journal of Cleaner Production 344 18–23, (2021).

33. Musa, A., Alozie, E., Suleiman, A., Ojo, J., Imoize, A.: A Review of Time-Based Solar Photovoltaic Tracking Systems. Information 14(4) 2–11, (2023).

34. Taheri, A.: Improving the performance of a nanofluid-based photovoltaic thermal module utilizing dual-axis solar tracker system: Experimental examination and thermodynamic analysis. Appl.Therm.Eng. 196 117178, (2021).

35. Krishnan, S., Umasankar, P., Mohana, P.: A smart FPGA based design and implementation of grid connected direct matrix converter with IoT communication," Microprocessors and Microsystems 76 103–107, (2020).

36. Cuong, N. X., Nha, V. Q., & Hong, N. T. (2018). A simplified calculation method of electric linear actuators for single-axis sun tracker. Hue University Journal of Science: Natural Science, 127(1D), 47-54.

37. Alexandru, C., "Simulation and Optimization of a Dual-Axis Solar Tracking Mechanism," *Mathematics*, vol. 12, p. 1034, 2024, doi: 10.3390/math12071034.

38. Keo, C., Srang, S., and Seng, R., "Performance Investigation of Low-Cost Dual-Axis Solar Tracker Using Light Dependent Resistor," *International Journal of Robotics and Control Systems*, vol. 3, no. 4, pp. 853–869, 2023. [Online]. Available: https://ijrcs.org. [Accessed: Nov. 15, 2024].

39. Flores-Hernández, D. A., Islas-Estrada, L. R., and Palomino-Resendiz, S. I., "A Novel Tracking Strategy Based on Real-Time Monitoring to Increase the Lifetime of Dual-Axis Solar Tracking Systems," *Applied Sciences*, vol. 14, no. 18, p. 8281, 2024. [Online]. Available: https://doi.org/10.3390/app14188281.

40. Aji, M. M., Gamiya, B. G., Olomowewe, A. T., Ohikere, F. A., Umar, S. S., and Thomas, S., "Design and Simulation of Dual-Axis Solar Tracking Systems," *2021 1st International Conference on*

Multidisciplinary Engineering and Applied Science (ICMEAS), Abuja, Nigeria, 2021, pp. 1–4, doi: 10.1109/ICMEAS52683.2021.9692361.

41. Abdelghany, E. S., Farghaly, M. B., Almalki, M. M., Sarhan, H. H., & Essa, M. E. S. M. (2023). Machine learning and iot trends for intelligent prediction of aircraft wing anti-icing system temperature. Aerospace, 10(8), 676.